



# Optical properties of copper clusters in zeolite 4A with surface enhanced Raman spectroscopy applications

J. E. Leal-Perez<sup>1</sup> · J. Flores-Valenzuela<sup>1</sup> · M. Cortez-Valadez<sup>2</sup> · A. Hurtado-Macías<sup>3</sup> · R. A. Vargas-Ortiz<sup>1</sup> · J. G. Bocarando-Chacon<sup>4</sup> · J. L. Almaral-Sánchez<sup>1</sup>

Received: 19 February 2022 / Accepted: 18 June 2022

© The Author(s), under exclusive licence to Springer-Verlag GmbH, DE part of Springer Nature 2022

## Abstract

In this study, we used the ion exchange properties of zeolite 4A to stabilize copper ionic species. These species showed absorption bands in the ultraviolet region between 210 and 320 nm. Complementarily, DFT (Density-Functional Theory) at different levels of approximation was employed in combination with the LANL2DZ (Los Alamos National Laboratory 2 double zeta) and SDD (Stuttgart/Dresden) basis sets to find hints of optical absorption behavior associated with electronic transitions. The copper clusters in ZA were evaluated as SERS (Surface-Enhanced Raman Spectroscopy) substrate using pyridine (Py) and methylene blue (MB) molecules. Additionally, molecular descriptors as electron transfer factor, electronegativity and global hardness were considered to study the charge transfer between the molecular systems and the ionic copper species. The DFT calculations suggest that the  $Cu_3^+$  cluster manifests optically. The molecular descriptors allowed to identify the effect of charge transfer from the analyte to the cluster, specifically toward the LUMO or higher energy orbitals, and the systems obtained showed capacity as SERS substrates, evaluated on Py and MB.

**Keywords** Copper ions · Chemical enhancement mechanism · Zeolite 4A · Theoretical and experimental analysis

## 1 Introduction

Zeolites are hydrated aluminosilicates and they feature the characteristic to exchange cations [1]. In addition, they can host different structures in their matrix, and it makes them attractive for different applications [2]. Zeolite 4A (ZA) has  $Na^+$  as the only exchange ion, which facilitates its study [3]. The different active sites in ZA provide conditions for the ion exchange or structure hosting [4].

Surface-enhanced Raman scattering (SERS) is used for its high sensitivity, selectivity and reliability in the traces detection of chemical molecules [5–7]. When a molecule interacts with the SERS substrate, it amplifies the Raman signal by several orders of magnitude. This effect is associated with two mechanisms: (1) electromagnetic effect (EM), which consists of an intensification of the Raman spectrum caused by the scattered radiation due to the metal surface and (2) chemical effect (CE), based on charge transfer and/or complex formation between the absorbed molecules and the substrate surface [8]. SERS substrates are made of Ag, Au or Cu and they incorporate metallic elements [9–13]. Additionally, there are reports of oxides such as: ZnO,  $Ag_xMo_yO_z$ ,  $Fe_2O_3$  and carbon composites with SERS applications [14–18]. There are currently few theoretical and experimental results in the literature on the SERS response of ionic species. However, the presence of ionic systems has been analyzed in some matrices, finding a promising increase in SERS activity [19].  $Ag^+$  ions have allowed the formation of complexes in molecules providing SERS active sites that contribute an enhancement factor reaching up to  $10^7$  [20]. Recently, Lancu et al. analyzed the increase in the SERS effect due to the interaction of  $Ag^+$ ,  $Ca^{2+}$ ,  $Pb^{2+}$  and

✉ J. L. Almaral-Sánchez  
jalmaral@uas.edu.mx

<sup>1</sup> Facultad de Ingeniería Mochis, Universidad Autónoma de Sinaloa, Fuente de Poseidón y Prol. Ángel Flores S/N, Fracc. Las Fuentes, 81223 Los Mochis, Sinaloa, México

<sup>2</sup> Departamento de Investigación en Física, CONACYT, Universidad de Sonora, 83000 Hermosillo, Sonora, México

<sup>3</sup> Centro de Investigación en Materiales Avanzados S.C, Department of Metallurgy and Structural Integrity, National Nanotechnology Laboratory, 31109 Chihuahua, Chihuahua, México

<sup>4</sup> Universidad Tecnológica de Querétaro, (Autonomous), 76148 Santiago de Querétaro, Querétaro, Mexico

$\text{Al}^{3+}$  ions with uric acid, salicylic acid, and fumaric acid as analytes [21]. They have attributed the SERS effect to the chemical enhancement mechanism, specifically to the charge transfer effect. In addition, theoretical results confirm the presence of the SERS effect when  $\text{Ag}^+$  ions interact with molecules such as adenosine and adenine [22, 23]. Through density functional theory (DFT), the SERS behavior has been analyzed in clusters with few metal atoms, modifying the cluster charge. [24], unlike other theories, such as the frameworks of finite-difference time-domain theory (FDTD), which simulates scattering cross-sections and presents a good approximation for nanostructured systems of larger size  $\sim 100$  nm [25].

On the other hand, the incorporation of metal ions ( $\text{Ag}^+$ ) in the zeolite cavities has allowed to obtain SERS substrates for the detection of molecules such as tris(2,2'-bipyridyl) ruthenium(II) chloride ( $\text{RuBpy}$ ) and rhodamine 6G (R6G) at low concentrations, even without the presence of nanoparticles [26]. Furthermore, by introducing metal ions into the zeolite cavities, SERS substrates are obtained that exhibit this effect at temperatures about  $450^\circ\text{C}$  [27]. Such substrates can be used for in situ SERS monitoring of temperature-dependent catalytic reactions in unconventional ranges.

In this study, the ZA-copper ionic complex was evaluated as SERS substrate. The DFT modeling used in this work tries to provide a theoretical hypothesis of the SERS effect in the  $\text{Cu}_3^+-\text{Py}$  and  $\text{Cu}_3^+-\text{MB}$  interacting systems. The ZA-copper complex obtained in this work can contribute to the low-cost SERS sensors, cost-competitive with those currently available focus on Methylene Blue and Pyridine.

## 2 Materials and methods

Two samples of 5 g zeolite 4A (ZA) powder (Sigma-Aldrich) were immersed in 20 ml of deionized water for hydration over 24 h. Complementary, two solutions (0.03 and 0.1 M) of copper sulfate ( $\text{CuSO}_4 \cdot 5\text{H}_2\text{O}$ , 99.5%, Faga Lab) were prepared. Both hydrated ZA and copper sulfate solution were separately placed in a thermal bath at  $50^\circ\text{C}$ . Subsequently, we added the copper sulfate solution to the ZA under magnetic stirring treatment and at a constant temperature. Afterwards, the stirring process continued for 25 min, and the sample was filtered with deionized water. This process was repeated 3 times, and then the mixture was dried at room temperature for 24 h. Finally, we obtained the composite ZA + Cu0.03 ( $\text{ZA-Cu}_{(0.03)}$ ). This process was repeated for the 0.1 M solution of copper sulfate, obtained the ZA + Cu0.1 composite ( $\text{ZA-Cu}_{(0.1)}$ ).

### 2.1 Sample preparation for SERS

The methodology for the SERS application was applied in a previous work [28]. Three vials were prepared with 2 ml of pyridine (Py) ( $5 \times 10^{-5}$  M, Sigma-Aldrich), to add 0.01 g of: ZA,  $\text{ZA-Cu}_{(0.03)}$  and  $\text{ZA-Cu}_{(0.1)}$ , respectively. Then, they were kept at rest for 5 min and subsequently measured by Raman spectroscopy, obtaining the Py-ZA, Py-ZA-Cu $_{(0.03)}$  and Py-ZA-Cu $_{(0.1)}$  systems.

For the SERS effect on methylene blue (MB) (Supelco Corp.), the previous step was carried out in the same procedure, obtaining MB-ZA, MB-ZA-Cu $_{(0.03)}$  and MB-ZA-Cu $_{(0.1)}$ .

### 2.2 Characterizations

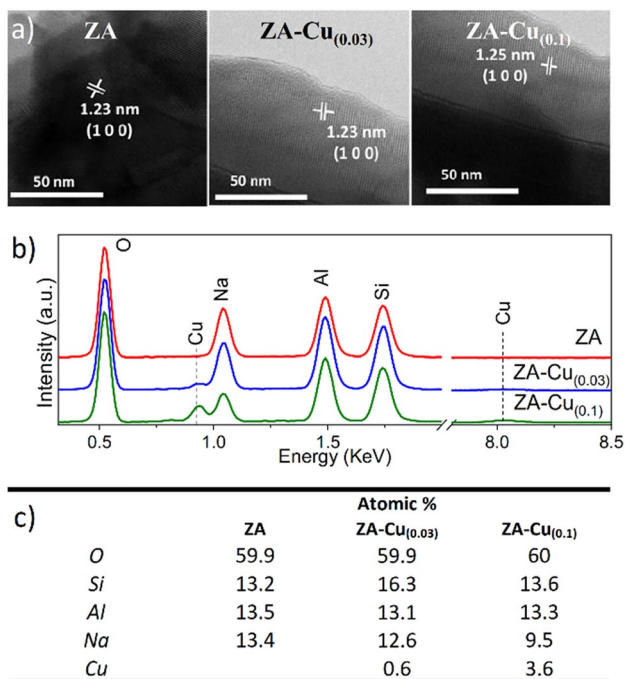
The chemical composition and crystalline planes were analyzed by transmission electron microscopy (EDS-TEM and HRTEM) using JEOL JEM-2200FS + Cs equipment. Optical absorption spectra were obtained using a Perkin Elmer Lambda 19 UV-Vis spectrometer. The SERS effect was evaluated using the Horiba LABram HR Evolution Raman spectrometer (with AFM, AIST-NT coupled).

### 2.3 Theoretical calculations

Theoretical calculations were developed using the DFT (density functional theory) through the B3LYP (Becke-3 Parameter-Lee-Yang-Parr), B3PW91 (Becke-Perdew-Wang 1991), and mPW1PW91 (Barone and Adamo's Becke-style one parameter functional with modified Perdew-Wang exchange and Perdew-Wang 91 correlation) approximations levels. These in combination with the LANL2DZ (Los Alamos National Laboratory 2 double zeta) and SDD (Stuttgart/Dresden pseudopotentials) basis set, integrated into the Gaussian 09 software [29]. The structures considered were first optimized to the local minimum, verifying that only positive frequencies were obtained in the vibrational spectrum. The standard SCF convergence criterium ( $10^{-8}$  au) was used. The same standard criterium for Maximum and RMS Force were used ( $10^{-4}$  au). Additionally, a  $10^{-3}$  au criterium was applied for Maximum and RMS displacement. Subsequently, the TD-DFT (Time Dependent Density Functional Theory) was used to calculate the UV-Vis spectrum. The molecular descriptors allowed us to elucidate the behavior of the SERS effect in a first approximation. By predicting the energy levels of the molecular orbitals (HOMO-LUMO), we were able to determine the electron transfer fraction ( $\Delta N$ ) between the  $\text{Cu}_3^+-\text{Py}$  and  $\text{Cu}_3^+-\text{MB}$  systems. The  $\Delta N$  is related to the chemical enhancement mechanism.

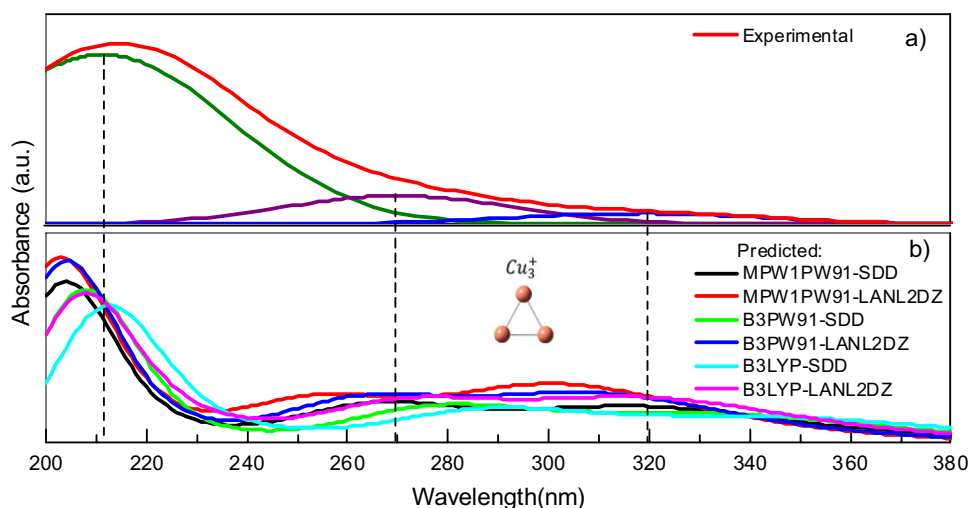
### 3 Results and discussion

Figure 1 shows (a) HRTEM, (b) EDS and (c) elemental composition of ZA, ZA-Cu<sub>(0.03)</sub> and ZA-Cu<sub>(0.1)</sub>. In (a), for ZA and ZA-Cu<sub>(0.03)</sub> can be observed the crystalline planes with an interplanar distance of 1.23 nm, corresponding to the Miller index (1 0 0), characteristic of ZA with a cubic crystalline system and space group Pm-3 m (indexed in PDF # 01-074-1183), unchanged by Cu presence. In ZA-Cu<sub>(0.1)</sub>, a slightly larger interplanar distance was obtained at 1.25 nm,



**Fig. 1** a HRTEM micrographs, b EDS and c elemental composition of ZA, ZA-Cu<sub>(0.03)</sub> and ZA-Cu<sub>(0.1)</sub> respectively.

**Fig. 2** Optical absorption spectra of a experimental and b theoretical ZA-Cu<sub>3</sub><sup>+</sup> complex by several DFT levels of approximation



it can be attributed to the modification of the ZA crystal lattice caused by the hosted copper ions, due to having a high concentration of copper. We assume this because only the ZA planes are observed denoting the absence of possible nanoparticles. In (b) shows the characteristic elements O, Al, Si, and Na for ZA, on the other hand, in ZA-Cu<sub>(0.03)</sub> and ZA-Cu<sub>(0.1)</sub> a Cu peak is observed. In (c) shows the characteristic elements of ZA, according to its molecular structure, Na<sub>12</sub>[Al<sub>12</sub>Si<sub>12</sub>O<sub>48</sub>]·27H<sub>2</sub>O [30]. A stoichiometry of 1:1:1 between Al, Si and Na must be satisfied. In ZA-Cu<sub>(0.03)</sub> and ZA-Cu<sub>(0.1)</sub> observed that Al and Si are preserved in their equivalence, moreover, adding the values of Na and Cu, it is possible to obtain the equivalence 1:1:1. Based on this, we can assume that cation exchange is carried out, since no copper nanoparticles are observed in (a), we suppose that this exchange occurs in the framework of an early stage of growth, limited to obtaining species in the cavity. Ion exchange in zeolite is a not well-understood process. With cavity sizes approximate 4 Å and 7 Å, α-cage and β-cage, respectively.

Figure 2 shows the experimental optical absorption spectra of ZA-copper complex systems, obtained according to the Kubelka–Munk model [31]. The UV–Vis spectrum shows the absence of absorption bands (approximately 500–600 nm) associated with copper nanoparticles. (Fig. S1, Supplemental information). Figure 2a includes a deconvolution of the experimental spectrum (green, purple, and blue lines). We can assume that the optical behavior is associated with copper species in the ZA matrix. Therefore, we evaluated the TD-DFT under the B3LYP, B3PW91, and MPW1PW91 approximation levels combined with the LANL2DZ and SDD basis sets on Cu<sub>3</sub><sup>+</sup> (Fig. 2b). The first 40 transition states were considered for all approximation levels. Therefore, the absorption lines correspond to the allowed transitions between the ground state S<sub>0</sub> and the excited states S<sub>n</sub>, n = 1 to 40. For

the  $Cu_3^+$  system, the  $S0 \rightarrow S39$  transition was located close to 210 nm for the considered approximation levels. The associated electronic transition from the  $S0 \rightarrow S24$  state shows absorption bands between 250 and 300 nm. Both  $S0 \rightarrow S39$  and  $S0 \rightarrow S24$  transitions exhibited susceptibility according to the approximation level used. When MPW1PW91/LANL2DZ was used, a shift toward higher energies was observed. The occupation of the electronic states has shown in the LDOS spectra. (Fig. S2, Supplemental information).

Moreover, using B3LYP/SDD, absorption bands were observed at lower energies. The B3LYP/LANL2DZ level of approximation shows a better estimate of the location of absorption bands in the experimental UV–Vis spectrum. Other larger ionic systems were studied. However, their localized absorption bands at lower energies show significant differences concerning the results obtained experimentally. The theoretical details in Fig. 2 suggest that the experimentally obtained absorption band could have a contribution associated with ionic copper species. When a specific ionic system is obtained in a zeolite matrix, it could be used as SERS substrate. It is due to charge transfer effects between the studied molecule and the substrate. It occurs in the CEM (Chemical Enhancement Mechanism) framework [26, 32]. Previously, electronic transitions have been reported between the boundary orbitals of the analyte molecule (regularly pyridine) with metallic atomic systems, evidencing the charge transfer effects [33–35].

Furthermore, the SERS analysis was performed on Py and MB molecule as observed in Fig. 3. Figure 3a shows the Raman spectrum associated with Py (black line) with two characteristic bands identified as radial breathing modes and ring vibrations. The first one is located at  $990\text{ cm}^{-1}$  and the second one at  $1030\text{ cm}^{-1}$ . Both are susceptible to the SERS effect. The Raman spectrum of the Py-ZA interacting system (red line) has been included as a complement. In this case, we do not observe the SERS effect. In contrast, we found a slight attenuation. After including the copper ionic system in the ZA matrix interacted with Py, we observed an intensification of the Py vibrational bands. In the Py-ZA-Cu<sub>(0.1)</sub> sample (green line), we found evidence of the SERS effect.

Complementarily, when analyzing the SERS effect of substrate on MB, we observed similar behavior. Hence, we observed an attenuation degree of the characteristic MB bands in the Py-ZA system (Fig. 3b red line). The characteristic vibrational bands of the MB are located around  $445, 475, 1400,$  and  $1620\text{ cm}^{-1}$ . The first one is associated with the C–N skeleton deformation mode. In addition, the

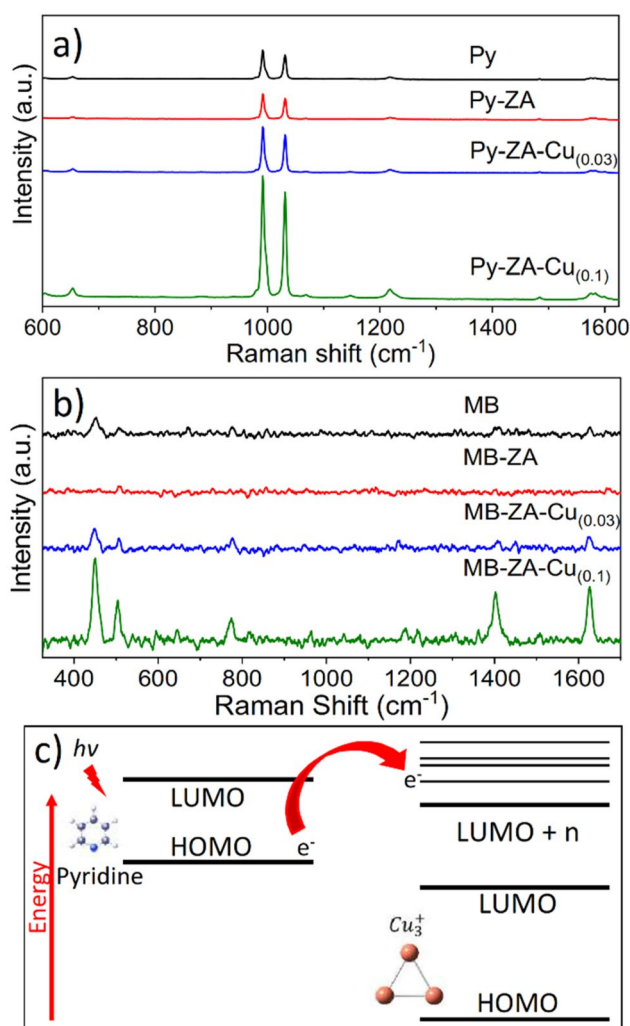


**Fig. 3** Raman spectra ZA-copper ionic complex in interaction with a Py, b MB and c Charge transfer scheme

band at  $475\text{ cm}^{-1}$  is associated with the in-plane bending vibrations of the thiazine group. [36]. The nearest band at  $1400\text{ cm}^{-1}$  and the other around  $1620\text{ cm}^{-1}$  are susceptible to the SERS effect. [37, 38]. These are associated with C–H bond deformation and C–C stretching, respectively [39]. We observe significant enhancement in the above bands only for MB-ZA-Cu<sub>(0.1)</sub> sample.

In addition, to study the charge transfer effect, it is worth using some molecular descriptors that provide some details of the electronic behavior. The measure tendency of an atom to attract a pair of bonding electrons is known as electronegativity. An important parameter is the electron transfer fraction ( $\Delta N$ ), this parameter is related to the electronegativity and the global hardness, represented by Pearson's method as:

$$\Delta N = \frac{\chi_{cluster} - \chi_{pyridine}}{2[\eta_{cluster} + \eta_{pyridine}]} \quad (1)$$

where  $\chi_{cluster}$  y  $\eta_{cluster}$  are electronegativity and global hardness parameters for the cluster, y  $\chi_{pyridine}$  y  $\eta_{pyridine}$  are the corresponding parameters for the molecule, respectively.

$$\text{Where } \chi = \frac{-HOMO - LUMO}{2} \text{ and } \eta = \frac{-HOMO - LUMO}{2} \quad (2)$$

The difference in the numerator, or the difference in electronegativities, will be responsible for the electron transfer. Electron transfer will occur from the low electronegativity molecule to another one with higher electronegativity. If  $\Delta N > 0$ , the electron transfer proceeds from the molecule to the cluster, and the opposite apply if  $\Delta N < 0$  [40]. However, this is considered an approximation to provide information on electronic behavior that can be used as a complement to obtain details of CEM behavior before intermolecular interaction studies. We consider the HOMO (− 6.93 eV), LUMO (− 1.79 eV) values of the Py reported [41] and the HOMO (− 12.01 eV) and LUMO (− 7.53 eV) values of the  $Cu_3^+$  obtained in this work for the same level of theory. Preliminarily, we can determine that the electronegativity  $\chi$  is lower for Py. Therefore, charge transfer should occur from the Py molecule to the  $Cu_3^+$  cluster. If we calculate  $\Delta N$  from Eq. (1), we could obtain a positive value to confirm the charge transfer direction, as observed in Fig. 3c. Therefore, incident radiation with the required energy would cause a transfer of the Py HOMO to the LUMO or higher energy orbitals of the ionic cluster. In the case of MB, with HOMO (− 5.524 eV) and LUMO (− 3.619 eV) values [42], a similar behavior could occur in the charge transfer on the MB molecule, i.e., it would apply from the HOMO of the MB to higher energy orbitals concerning to the LUMO of the cluster.

Additionally, Table 1 compares the structural parameters of the cluster.  $Cu_3^+$  obtained in this work and those reported in the literature. For the Cu-Cu bond distance, a minimum value of 2.30 Å has been reported by the VWN level of approximation combined with the DZVP basis set [43]. We obtained a maximum value in the Cu-Cu bond for the hybrid levels of approximation considered with the LANL2DZ basis set. This value of 2.39 Å agrees with the one reported by Fernandez et al. for the GGA (Generalized Gradient Approximation) PBE pseudopotential [44]. Complementary, the point group symmetry usually corresponds to  $D_{3h}$ , depicting an equilateral triangle.

## 4 Conclusion

The macroscopic parameters proposed for the synthesis process led to ZA-copper complex systems, possibly identified as ionic species. Theoretical clues suggest that the  $Cu_3^+$  cluster manifests optically. The experimental absorption bands of this type of species were positioned in the ultraviolet region. These were found in close regions to the electronic transitions obtained theoretically by the different levels of DFT approximation. The B3LYP level of approximation combined with the LANL2DZ basis set shows the best approximation. On the other hand, the ZA-copper complex systems obtained showed capacity as SERS substrates evaluated on Py and MB analytes. In both cases, a higher enhancement was achieved for copper concentrations (0.1 M). The molecular descriptors allowed to identify the charge transfer effect from the molecule to the cluster, specifically toward the LUMO or higher energy orbitals. The substrates obtained can be applied as SERS substrates to detect trace chemical compounds of MB or Py at a low cost and with a low toxicity level using low concentrations of the copper precursor.

**Table 1** Structural parameters of  $Cu_3^+$  cluster obtained by several DFT approximations levels

Level of Theory	Basis set	$R_{Cu-Cu}$ (Å)	Point group symmetry	Pseudopotentials	Reference
B3LYP	6-311G	2.32	$D_{3h}$	Hybrid	[45]
PBE	FLCNA <sup>b</sup>	2.39	$D_{3h}$	GGA	[44]
VWN	63,321/531 <sup>3</sup> /411	2.28	$D_{3h}$	Local	[46]
VWN	DZVP	2.30	$D_{3h}$	Local	[43]
BLYP	6-311 + G(d)	2.38	$D_{3h}$	Hybrid	[47]
B3LYP	LANL2DZ/SDD	2.39/2.36	$D_{3h}$	Hybrid	This work
B3PW91	LANL2DZ/SDD	2.39/2.35	$D_{3h}$	Hybrid	
mPW1PW91	LANL2DZ/SDD	2.39/2.35	$D_{3h}$	Hybrid	

<sup>b</sup>Flexible linear combinations of numerical (pseudo) atomic

\*It is part of the Huzinaga notation, for the orbital basis set for Cu

**Supplementary Information** The online version contains supplementary material available at <https://doi.org/10.1007/s00339-022-05785-6>.

**Acknowledgements** The authors acknowledge the support of the DGIP of the Universidad Autónoma de Sinaloa (UAS), for the financial support through the PROFAPI2015/100 Project, to the CONACYT for their support of scholarships No. 444248, to the Centro de Investigación en Materiales Avanzados-Chihuahua for its support in the infrastructure and equipment, and to UNISON/ACARUS, for its support in the computational resources for this investigation. The author M. Cortez-Valadez is grateful for the support of the INVESTIGADORES POR MEXICO-CONACYT program and project A1-S-46242 funded by CONACYT for the development of this work.

**Author contributions** All authors contributed to the study conception and design. JE Leal-Perez, JFV and JLAS: performed the material preparation and data collection. The author MCV: performed the SERS analysis. JELP and JFV, MCV: written the first draft of the manuscript. AHM, RAVO, and JGBC: contributed to results analysis. All authors commented on previous versions of the manuscript, also, read and approved the final manuscript.

**Funding** The research was supported by A) The DGIP at the Universidad Autónoma de Sinaloa (UAS) through the PROFAPI2015/100 Project, B) The Consejo Nacional de Ciencia y Tecnología (CONACYT) for their support of scholarships No. 444248, C) The Centro de Investigación en Materiales Avanzados, S.C. (CIMA), for its support in the infrastructure and equipment, and D) UNISON/ACARUS, for its support in computational resources. E) The author M. Cortez-Valadez is grateful for the support of the INVESTIGADORES POR MEXICO-CONACYT program and project A1-S-46242 funded by CONACYT for the development of this work.

**Availability of data and material** Not applicable for that section.

**Code availability** Not applicable for that section.

## Declarations

**Conflict of interest** The authors have no relevant financial or non-financial interests to disclose. The authors have no conflicts of interest to declare that are relevant to the content of this article.

## References

- N. Eroglu, M. Emekci, C.G. Athanassiou, *J. Sci. Food Agric.* **97**, 3487 (2017). <https://doi.org/10.1002/jsfa.8312>
- A. Sachse, J. García-Martínez, *Chem. Mater.* **29**, 3827 (2017). <https://doi.org/10.1021/acs.chemmater.7b00599>
- K.D. Mondale, R.M. Carland, F.F. Aplan, *Miner. Eng.* **8**, 535 (1995). [https://doi.org/10.1016/0892-6875\(95\)00015-1](https://doi.org/10.1016/0892-6875(95)00015-1)
- C.D. Chudasama, J. Sebastian, R.V. Jasra, *Ind. Eng. Chem. Res.* **44**, 1780 (2005). <https://doi.org/10.1021/ie0493331>
- N.X. Dinh, T.Q. Huy, L. Van Vu, L.T. Tam, A.T. Le, *J. Sci. Adv. Mater. Devices* **1**, 84 (2016). <https://doi.org/10.1016/j.jsamd.2016.04.007>
- Z. Lin, L. He, *Curr. Opin. Food Sci.* **28**, 82 (2019). <https://doi.org/10.1016/j.cofs.2019.10.001>
- Y.J. Oh, M. Kang, M. Park, K.H. Jeong, *Biochip J.* **10**, 297 (2016). <https://doi.org/10.1007/s13206-016-0406-2>
- Q. Huang, J. Wang, W. Wei, Q. Yan, C. Wu, X. Zhu, *J. Hazard. Mater.* **283**, 123 (2015). <https://doi.org/10.1016/j.jhazmat.2014.09.021>
- Y. Sun, T. Li, *Anal. Chem.* **90**, 11614 (2018). <https://doi.org/10.1021/acs.analchem.8b03067>
- X.H. Pham, E. Hahm, T.H. Kim, H.M. Kim, S.H. Lee, S.C. Lee, H. Kang, H.Y. Lee, D.H. Jeong, H.S. Choi, B.H. Jun, *Nano Res.* **13**, 3338 (2020). <https://doi.org/10.1007/s12274-020-3014-3>
- X. Yan, M. Wang, X. Sun, Y. Wang, G. Shi, W. Ma, P. Hou, *Appl. Surf. Sci.* **479**, 879 (2019). <https://doi.org/10.1016/j.apsusc.2019.02.072>
- Y. Tang, X. Chen, Y. Lv, Z. Wu, F. Chen, Z. Chen, *J. Inorg. Organomet. Polym. Mater.* **28**, 251 (2018). <https://doi.org/10.1007/s10904-017-0703-9>
- C. Liu, J. Xu, H. Chen, *J. Inorg. Organomet. Polym. Mater.* **25**, 153 (2015). <https://doi.org/10.1007/s10904-014-0126-9>
- P. Dyakonov, K. Mironovich, S. Svyakhovskiy, O. Voloshina, S. Dagesyan, A. Panchishin, N. Suetin, V. Bagratashvili, P. Timashev, E. Shirshin, S. Evlashin, *Sci. Rep.* **7**, 1 (2017). <https://doi.org/10.1038/s41598-017-13087-8>
- X. Liang, N. Li, R. Zhang, P. Yin, C. Zhang, N. Yang, K. Liang, B. Kong, *NPG Asia Mater.* **13**, 1 (2021). <https://doi.org/10.1038/s41427-020-00278-5>
- X. Fu, F. Bei, X. Wang, X. Yang, L. Lu, *Mater. Lett.* **63**, 185 (2009). <https://doi.org/10.1016/j.matlet.2008.09.027>
- Y. Lin, Z. Xiaoming, *Mater. Lett.* **62**, 3764 (2008). <https://doi.org/10.1016/j.matlet.2008.04.059>
- A. Aarthi, M. Umadevi, R. Parimaladevi, G.V. Sathe, S. Arumugam, P. Sivaprakash, *J. Inorg. Organomet. Polym. Mater.* **31**, 1469 (2021). <https://doi.org/10.1007/s10904-020-01802-4>
- S.Y. Fu, P.X. Zhang, *J. Raman Spectrosc.* **23**, 93 (1992). <https://doi.org/10.1002/jrs.1250230206>
- T. Watanabe, O. Kawanami, K. Honda, B. Pettinger, *Chem. Phys. Lett.* **102**, 565 (1983). [https://doi.org/10.1016/0009-2614\(83\)87467-3](https://doi.org/10.1016/0009-2614(83)87467-3)
- S.D. Iancu, A. Stefanu, V. Moisoiu, L.F. Leopold, N. Leopold, *Beilstein J. Nanotechnol.* **10**, 2338 (2019). <https://doi.org/10.3762/bjnano.10.224>
- M. Muniz-Miranda, C. Gellini, M. Pagliai, M. Innocenti, P.R. Salvi, V. Schettino, *J. Phys. Chem. C* **114**, 13730 (2010). <https://doi.org/10.1021/jp103304r>
- R. Huang, L. Bin Zhao, D.Y. Wu, Z.Q. Tian, *J. Phys. Chem. C* **115**, 13739 (2011). <https://doi.org/10.1021/jp201977z>
- G. Cardini, M. Muniz-Miranda, M. Pagliai, V. Schettino, *Theor. Chem. Acc.* **117**, 451 (2007). <https://doi.org/10.1007/s00214-006-0176-3>
- Y.Y. Cai, S.S.E. Collins, M.J. Gallagher, U. Bhattacharjee, R. Zhang, T.H. Chow, A. Ahmadivand, B. Ostovar, A. Al-Zubeidi, J. Wang, P. Nordlander, C.F. Landes, S. Link, *ACS Energy Lett.* **4**, 2458 (2019). <https://doi.org/10.1021/acsenenergylett.9b01747>
- N. Liu, M. Gong, P. Zhang, L. Li, W. Li, R. Lee, *J. Mater. Sci.* **46**, 3162 (2011). <https://doi.org/10.1007/s10853-010-5199-4>
- P.K. Dutta, D. Robins, *Langmuir* **7**, 2004 (1991). <https://doi.org/10.1021/la00058a005>
- R. Britto Hurtado, M. Cortez-Valadez, L.P. Ramírez-Rodríguez, E. Larios-Rodríguez, R.A.B. Alvarez, O. Rocha-Rocha, Y. Delgado-Beleño, C.E. Martínez-Núñez, H. Arizpe-Chávez, A.R. Hernández-Martínez, M. Flores-Acosta, *Phys. Sect. At. Solid State Phys. Lett. A Gen.* (2016). <https://doi.org/10.1016/j.physleta.2016.05.052>
- R.K. and J.N.M. Frisch, G. Trucks, H. Schlegel, G. Scuseria, M. Robb, J. Cheeseman, G. Scalmani, V. Barone, B. Mennucci, G. Petersson, H. Nakatsuji, M. Caricato, X. Li, H. Hratchian, A. Izmaylov, J. Bloino, G. Zheng, J. Sonnenberg, M. Hada, M. Ehara, K. Toyota, R. Fuk, Gaussian 09, Revision D.01 (Gaussian Inc, Wallingford CT, 2009), p. 398.

30. S. Sugiyama, S. Yamamoto, O. Matsuoka, H. Nozoye, J. Yu, G. Zhu, S. Qiu, O. Terasaki, *Microporous Mesoporous Mater.* **28**, 1 (1999). [https://doi.org/10.1016/S1387-1811\(98\)00271-6](https://doi.org/10.1016/S1387-1811(98)00271-6)
31. P. Kubelka, F. Munk, *Z. Tech. Phys* **12**, 593 (1931)
32. C.E. Martínez-Nuñez, Y. Delgado-Beleño, M. Cortez-Valadez, N.S. Flores-López, M. Flores-Acosta, F.F. Castillón-Barraza, *Mater. Chem. Phys.* **211**, 150 (2018). <https://doi.org/10.1016/j.matchemphys.2017.12.075>
33. H. Nose, M.T. Rodgers, *J. Phys. Chem. A* **118**, 8129 (2014). <https://doi.org/10.1021/jp500488t>
34. B. Happ, A. Winter, M.D. Hager, U.S. Schubert, *Chem. Soc. Rev.* **41**, 2222 (2012). <https://doi.org/10.1039/c1cs15154a>
35. B. Drahoš, R. Herchel, Z. Trávníček, *Inorg. Chem.* **54**, 3352 (2015). <https://doi.org/10.1021/ic503054m>
36. S. Fateixa, M. Wilhelm, A.M. Jorge, H.I.S. Nogueira, T. Trindade, *J. Raman Spectrosc.* **48**, 795 (2017). <https://doi.org/10.1002/jrs.5136>
37. S. Santhoshkumar, E. Murugan, *Appl. Surf. Sci.* **553**, 149544 (2021). <https://doi.org/10.1016/j.apsusc.2021.149544>
38. R.V. William, G.M. Das, V.R. Dantham, R. Laha, *Sci. Rep.* **9**, 1 (2019). <https://doi.org/10.1038/s41598-019-47179-4>
39. H.T. Ali, A. Mateen, F. Ashraf, M.R. Javed, A. Ali, K. Mahmood, A. Zohaib, N. Amin, S. Ikram, M. Yusuf, *Ceram. Int.* **47**, 27998 (2021). <https://doi.org/10.1016/j.ceramint.2021.07.291>
40. S.K. Saha, P. Ghosh, A. Hens, N.C. Murmu, P. Banerjee, *Phys. E Low-Dimensional Syst. Nanostructures* **66**, 332 (2015). <https://doi.org/10.1016/j.physe.2014.10.035>
41. D.Y. Wu, M. Hayashi, Y.J. Shiu, K.K. Liang, C.H. Chang, Y.L. Yeh, S.H. Lin, *J. Phys. Chem. A* **107**, 9658 (2003). <https://doi.org/10.1021/jp0349511>
42. M. Khnifira, S. El Hamidi, A. Machrouhi, A. Mahsoune, W. Boumya, H. Tounsadi, F.Z. Mahjoubi, M. Sadiq, N. Barka, M. Abdennouri, *Desalin. Water Treat.* **190**, 393 (2020). <https://doi.org/10.5004/dwt.2020.25737>
43. K. Jug, B. Zimmermann, P. Calaminici, A.M. Köster, *J. Chem. Phys.* **116**, 4497 (2002). <https://doi.org/10.1063/1.1436465>
44. E.M. Fernández, J.M. Soler, I.L. Garzón, L.C. Balbás, in *Int. J. Quantum Chem (Am Phy Soc)*. (2005). <https://doi.org/10.1002/qua.20331>
45. M. Ichihashi, C.A. Corbett, T. Hanmura, J.M. Lisy, T. Kondow, *J. Phys. Chem. A* **109**, 7872 (2005). <https://doi.org/10.1021/jp0581577>
46. P. Calaminici, A.M. Kosten, N. Russo, D.R. Salahub, *J. Chem. Phys.* **105**, 9546 (1996). <https://doi.org/10.1063/1.472939>
47. G. Guzmán-Ramírez, F. Aguilera-Granja, J. Robles, *Eur. Phys. J. D* **57**, 49 (2010). <https://doi.org/10.1140/epjd/e2010-00001-4>

**Publisher's Note** Springer Nature remains neutral with regard to jurisdictional claims in published maps and institutional affiliations.